

# Stabilization of Neodymium Oxide Nanoparticles via Soft Adsorption of Charged Polymers

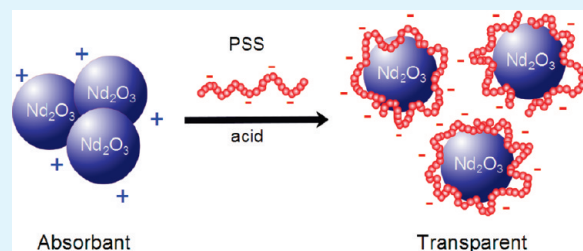
Annie Dorris,<sup>†</sup> Clémence Sicard,<sup>†</sup> Mark C. Chen,<sup>‡</sup> Arthur B. McDonald,<sup>‡</sup> and Christopher J. Barrett<sup>\*†</sup>

<sup>†</sup>Department of Chemistry, McGill University, Montreal, Canada

<sup>‡</sup>Department of Physics, Engineering Physics and Astronomy, Queen's University, Kingston, Canada

**ABSTRACT:** In this work, two synthetic polyelectrolytes, PSS and PAH, are employed as strong adsorbed surfactants to disperse and stabilize neodymium oxide nanoparticles. The acid–base equilibria of the oxide surfaces of the particles were investigated under different pH conditions in the absence and presence of polyelectrolytes, to optimize particle stabilization through enhancement of the effective repulsive surface charges. Surface charge amplification of a 3:5 ratio was achieved to permit improved particle transparency of 100-fold in visible wavelengths in neutral and acidic pH regimes, and a stable 10-fold surface charge amplification was achieved under basic pH conditions. The potential of polyelectrolytes as stabilizing agents for neodymium oxide NPs in large-scale particle physics experiments requiring extremely high optical transparency over long path length is evaluated based on optical absorbance and particle stability.

**KEYWORDS:** neodymium oxide, nanoparticles, poly(4-styrene sulfonate), polyelectrolyte stabilization, self-assembly of polyelectrolytes, rare-earth elements, neutrino detection materials



## INTRODUCTION

Neodymium oxide nanoparticles (Nd NPs) have gained much recent interest as optical and magnetic nanomaterials for various applications due to their unique optical properties. The contracted nature of the Nd 4f orbitals shielded by the 5s and 5p shells, common to all lanthanides, has a substantial effect on their physical properties. On the smallest length scale, below 10 nm, neodymium compounds acquire additionally interesting size-dependent quantum properties and well-defined secondary morphologies which are highly desired for a variety of size and surface-driven applications including photonics<sup>1</sup> and advanced NP-based materials,<sup>2,3</sup> surface catalytic systems,<sup>4</sup> and protective coatings.<sup>5</sup> Past lanthanide particle research was primarily focused on cerium-based NPs because of their high potential application in catalysis.<sup>6</sup> However, attention has most recently shifted to the preparation and characterization of other lanthanide NPs such as neodymium oxide, due to superior properties for some specific quantum applications. Most of these applications require nanoparticles of ultrafine powders with particle sizes of much less than 100 nm, and for some of the most interesting recent proposed applications, particle size is required to be less than 10 nm, or even 3–5 nm. High-quality neodymium oxide NPs with narrow size distributions in this extremely small size scale with various morphologies can now be prepared via solvothermal<sup>7</sup> or hydrothermal<sup>8</sup> processes. These ultrasmall NP materials are however far more susceptible to aggregation and destabilization as a consequence of their high surface energy and reactivity, preventing them from forming stable colloidal dispersions in solution, and rendering them unsuitable for some of the most interesting quantum applications, as they self-assemble back to 100 nm+ size aggregates in solution. This large-scale aggregation also deprives

the materials of their unique physical and chemical properties gained at the nanosize level, which differs greatly from those of bulk materials, and removes the optical transparency crucial to some of the key applications, due to scattering.

The present study was undertaken to investigate the optical properties of Nd NPs for possible use in the SNO+ experiment, an extension of the Sudbury Neutrino Observatory (SNO) experiment.<sup>9</sup> The SNO experiment used 1000 tonnes of ultra-pure heavy water observed by about 9500 light sensors in a large cavity excavated 2 km underground in Vale's Creighton mine near Sudbury, Ontario, Canada. In this deep and ultraclean location, shielded from cosmic ray particles, the SNO experiment detected neutrinos produced by nuclear reactions powering the sun and was able to demonstrate clearly<sup>10</sup> that the neutrinos changed their type, implying that they have a finite mass. This result requires modifications to the Standard Model for Elementary Particles and also confirms that current models of the Sun are very accurate. The SNO+ detector is under construction and will replace the heavy water in the central transparent acrylic sphere with linear alkylbenzene (LAB) and dissolved fluorophors providing a liquid scintillator with substantially higher light output than the Cerenkov processes generating light in the SNO experiment. For the first phase of the experiment, it is planned to add a ton or more of natural neodymium in order to look for neutrinoless double beta decay from the isotope <sup>150</sup>Nd. This rare radioactive process, if observed, would indicate that neutrinos are their own antiparticle (Majorana particles) and

Received: April 27, 2011

Accepted: July 15, 2011

Published: July 15, 2011

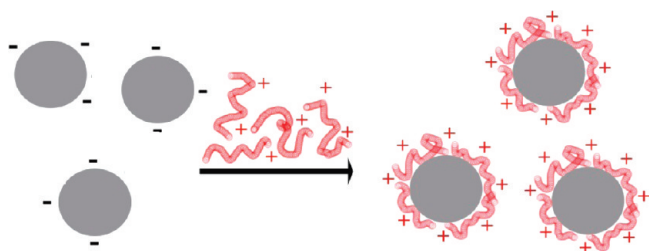


**Figure 1.** Basic mechanism of negatively charged nanoparticles being stabilized by the charge amplification because of soft adsorption of polycations.

would enable a determination of the absolute mass of the lightest neutrino.

The present work was initiated to examine the optical properties and stability of Nd NPs with diameters of about 5 nm to determine the amount of Nd that could be suspended in the liquid scintillator for the SNO+ experiment without unduly reducing the light transmission reaching the light sensors outside the 12 m diameter acrylic vessel holding the liquid scintillator. At such NP diameters, the amount of Rayleigh scattering is not expected to limit the experiment and the principal questions are (1) the optical absorption between wavelengths of about 350 and 450 nm and (2) the full dispersion and long-term stability of the NPs without aggregation or removal from suspension.

For dissolved Nd compounds, the principal absorption lines in the region from 350 to 450 nm arise from atomic absorption via the Nd 4f orbitals shielded by the 5s and 5p shells. Whereas similar absorption may occur for Nd NPs, these investigations were undertaken to determine if the condensed matter effects in the nanoparticles would have any positive effect on the absorption in the region of interest, perhaps enabling a larger amount of Nd to be suspended in the liquid scintillator without reduction in the light reaching the light sensors in SNO+. The objective for optical absorption in the nanoparticles would be to disperse more than 0.1% of Nd by weight while retaining absorption lengths in excess of 6 m in the Nd plus LAB scintillator for the 350–450 nm wavelength region.

The strong basic character of neodymium oxide and its weak solubility in water and organic solvents have traditionally made the preparation of stable colloidal suspensions of Nd NPs quite challenging. Only a few approaches have been attempted to disperse neodymium NPs, such as the direct chemical surface modification of the oxide,<sup>11</sup> and the formation of neodymium microemulsion from ionic surfactants.<sup>12</sup> Although the use of commercial polyelectrolytes to stabilize colloidal suspensions due to soft ionic adsorption (Figure 1) is a very common general trend in materials chemistry, the stabilization of neodymium oxide NPs in particular by this approach has not been reported in the literature because of the difficulty in soft ionic layering of charged polymers onto particles of the same size-scale as the polymer coils, which tend to desorb reversibly if not matched optimally to the underlying inorganic surface chemistry. Since neodymium oxide NPs possess a high natural surface charge which can be controlled with pH, further electrostatic stabilization via the self-assembly of polyelectrolytes to reverse and amplify is explored here. Moreover, the low cost and excellent transparency in the visible region of synthetic polyelectrolytes makes them highly appealing for this application, initially studied here in water, but with the eventual goal of transfer to LAB.

The layering and multilayering of polyelectrolytes onto metal and metal-inorganic surfaces is a simple yet highly successful process now common in industry,<sup>13</sup> whereby adsorption is due to “soft” interactions only (reversible ionic, not covalent) to a stable thermodynamic minimum configuration on the surface in excellent coverage, yet the large number of attachment points effectively renders the entire chain adhered with high stability over time, temperature, and solvent conditions under environmental, experimental, and most noncontact device conditions. Further to the layering onto flat surfaces, our group at McGill has worked toward adapting and optimizing this layering and multilayering of PEs onto the curved surfaces of colloidal NPs of various metals and inorganics,<sup>14,15</sup> with similar success in stability and control of layer coverage and charge reversal using pH, salt content, concentration, temperature, and molecular weight of the polymer chains. Our previous work has extended stable layering and charge reversal control down to particles below 10 nm,<sup>15</sup> and development of the requisite characterization techniques to confirm the surface layer size and structure in these small systems, such as solid-state NMR, zeta potential electrophoresis, electron microscopies, and neutron scattering.<sup>16,17</sup> In most cases, significant charge reversal and net surface charge enhancement could be achieved after optimal surface treatment and subsequent layering conditions were found, which most often resulted in significantly improved colloidal stability and solution transparency, as NPs were thus rendered more stable individually, and did not aggregate.

In the past, some interactions of synthetic polymers with lanthanide salts have been investigated, as polymers were used as a source of stabilization in some fluorescent studies.<sup>18–22</sup> Interactions between neodymium and poly(styrene sulfonate) have also been recently exploited in the fabrication of polyelectrolyte films doped with Nd(III).<sup>23,24</sup> However, these studies have focused exclusively on the interactions between polymers and lanthanide salts in their ionized form. In this work we propose to investigate the interactions of two commonly used polyelectrolytes, poly(styrene sulfonate) and poly(allylamine hydrochloride) with commercially available Nd oxide NPs. The influence of polyelectrolytes on the surface charge of the nanoparticles is investigated under a wide range of pH conditions, confirmed by measurement of the effective net surface charge via Zeta Potential Electrophoresis. Moreover, morphologies, aggregation states, and transparencies of Nd oxide NP solutions with and without the presence of polyelectrolytes are examined. In addition to the more applied end goal of stabilizing Nd NPs for suitability for the SNO+ experiment, there is also a more fundamental scientific desire to gain valuable insight into the surface chemistry of neodymium oxide, as many ongoing questions and curiosities concerning their surface and solution properties remain unanswered even after many decades. Therefore, the aim of this work is to compare and understand the behavior of interactions between a strong polyanion and a weak polycation with neodymium oxide nanoparticles under different pH conditions, and to evaluate their potential as stabilizing agents with high transparency criteria, using a simple and low-cost process performed under ambient conditions that could be scaled up indefinitely.

## EXPERIMENTAL SECTION

**Materials.** Neodymium oxide nanoparticle powder with diameters of 10 nm, Poly(styrene sulfonate) (PSS) with a  $M_w$  of 17 000 g/mol and

Poly(allylamine hydrochloride) (PAH) with a  $M_w$  of 15 000 g/mol were purchased from Sigma-Aldrich Chemical Co. (USA). Polydispersity data was not supplied by Sigma-Aldrich, but was measured by GPC to be approximately 1.5. Water purified to high resistivity (18.2 M $\Omega$ ) was used for all sample preparation and characterization experiments and was obtained using a mili-Q water system (Milipore Corporation, USA).

**Sample Preparation.** Colloidal suspensions of neodymium oxide were prepared by adding 10 mg of Nd<sub>2</sub>O<sub>3</sub> solid powder to 10 mL mili-Q water under vigorous stirring. The pH of the solution was tuned by using either a dilute NaOH 0.1 M solution or a dilute HCl 0.1 M solution. Due to the long equilibration times required by this acidification process, titration with HCl was performed at a very slow rate of 1 drop per 15 s. The acidified solutions were left to equilibrate for 24 h before the final pH and zeta potential were measured. During the titration, care was taken to ensure that the pH of the sample did not drop below 2.5, conditions leading to precipitation of a pink NdCl<sub>3</sub> aggregated product. No extra salt ions were added beyond the usual background levels, and acid counterion Cl. Electron microscopy showed these aggregates to exhibit an extremely wide range of nonuniform sizes, up to hundreds of nanometers and micrometers in some cases. In the case where polyelectrolyte interactions were investigated, a volume of 15 mL of PAH 5 mg/mL or a volume of 25 mL of PSS 5 mg/mL solutions were added to 5 mL of the neodymium oxide solution under stirring. In the case of PAH, the appropriate volume to be added was determined based on calculations of complete surface coverage from previous surface coverage studies using ellipsometry, while the volume of PSS to be added was based on a previous polymer-coated NPs study,<sup>25</sup> where large excesses of polyelectrolyte were used. The pH of the suspensions was also controlled by using HCl 0.1 M and NaOH 0.1 M solutions.

**Absorbance Measurements.** The transparency of NP suspensions was monitored by measuring the inversely the absorbance of samples with UV–vis spectroscopy on a Cary 500 UV–visible spectrophotometer using 1 cm quartz cuvettes. Absorbance measurements were recorded on aliquots of 2.5 mL of samples without further dilutions.

**Electrophoretic Mobility (EPM) Measurements.** Zeta potentials ( $\zeta$ -potential) of all suspensions were measured on a Zeta Plus zeta potential analyzer (Brookhaven Instrument Corporation, New York). Samples holding between 0.2 and 1 mg/mL of Nd<sub>2</sub>O<sub>3</sub> were used for analysis and an average over 10 measurements was calculated for each sample.

**Particle Visualization.** Transmission Electron Microscopy (TEM) experiments were performed on a Philips CM200 microscope using an acceleration voltage of 200 kV. The point-to-point and line resolutions of the microscope were respectively 0.24 and 0.17 nm.

## RESULTS AND DISCUSSION

**Acid–Base Chemistry of Nd<sub>2</sub>O<sub>3</sub> NPs.** Before investigation of the interactions of polyelectrolytes with neodymium oxide NPs to evaluate their potential as stabilizing agents, the particularly complex surface properties of Nd<sub>2</sub>O<sub>3</sub> nanoparticles which complicate the interpretation of results needed to be understood. Therefore, the first step of this work is an attempt to correlate the previously reported acid–base chemistry of bulk Nd<sub>2</sub>O<sub>3</sub> to the surface charge behavior of Nd<sub>2</sub>O<sub>3</sub> that we can measure for NPs at the 10 nm length scale under various pH environments.

Neodymium oxide is a strong base, which is only slightly soluble in water. The most common structure of neodymium oxide is termed “type A” and is made of layers of (NdO)<sub>n</sub><sup>n+</sup> cationic units of the crystallographic space group  $P3\bar{m}1$ . This implies that the neodymium atom has a coordination number of seven and is therefore connected to four oxygen ligands belonging to the ONd<sub>4</sub> tetrahedra in the (NdO)<sub>n</sub><sup>n+</sup> layer, and to three

other oxygen atoms in between the layer at a longer distance.<sup>26</sup> The bonding between atoms is dominated by ionic interactions<sup>27</sup> because covalent and crystal field contributions<sup>28</sup> are relatively weak. When the oxide is in contact with vapor or liquid water, Nd<sub>2</sub>O<sub>3</sub> usually associates with three water molecules to form Nd<sub>2</sub>O<sub>3</sub>·3H<sub>2</sub>O or Nd(OH)<sub>3</sub>.<sup>29</sup> Due to their highly basic character the crystals also tend to adsorb carbon dioxide from ambient air to form carbonate groups.<sup>30</sup> In contrast to the hydration that is independent of the crystal surface area, the carbonation process is limited to the outer layer of the oxide. It is worth noting that in this work we consider that the surface composition of the oxide is the same at the nanoscale level. When the Nd<sub>2</sub>O<sub>3</sub> NPs are mixed with water, the pH of the solution is approximately 7.5 and the charge at the NP surface is positive. The surface charge at this pH is attributed to the crystal’s overall charge which becomes positive upon hydroxylation. Under these conditions, the neodymium oxide NPs form large aggregates, which are presented in Figure 3a. The particles are not spherical and no longer uniform in size as they prefer to form a network of irregular trigonal 3D particles in an array of interconnected units. Hydrogen-bonding between hydroxyl groups at the NP surface is a possible source of aggregation as the presence of H-bonding has been confirmed by FTIR.<sup>4</sup> It has also been mentioned in the literature that the prethermal history of NPs can affect their shapes.<sup>8</sup>

In an attempt to induce nanoparticle dispersion via surface acidification, hydrochloric acid was very slowly added to the NP solution. In principle, inorganic acids such as HCl and HNO<sub>3</sub> commonly dissolve neodymium oxides in solution but with slow addition and good stirring, the acid instead appears to titrate the surface quantitatively, not reducing the pH to that leading to acidic dissolution, and reducing the aggregation by fragmenting the large aggregates. The pH was monitored during the HCl addition process to assess the titration end-point, and thus prevent the pH from dropping to very low values where neodymium is fully ionized. A master pH titration curve was thus obtained (presented in Figure 2a) and aliquots of acidified neodymium oxide NPs were withdrawn at different stages of the acidification process corresponding to different observable phases of visual transparency (A–F) to be analyzed by UV–vis spectroscopy (Figure 2b) zeta potential (Figure 2c), and TEM (Figure 3).

Prior to the addition of any acid (sample A), the pH of the neodymium colloidal solution is the original 7.5 (this value usually lies between pH 7.5 and 8.5 depending on atmospheric conditions) and the visible appearance of the solution is strongly cloudy. Large particles remain suspended in solution as long as there is vigorous stirring, otherwise they settle to the bottom gravitationally. When HCl is slowly added to the solution (B), the neodymium NP suspension gradually becomes less cloudy (B to C), whereas the pH of the solution remains neutral, implying that all of the acid added is consumed by the particle surface, and not free in solution to lower the pH. Following the dramatic change in pH (D) the solution becomes completely transparent visually to the observer (E to F). UV–vis spectra of NP solutions recorded by removing aliquots at these various stages of the acidification reaction are presented in Figure 2b. As expected, the scattering losses gradually decrease with pH as the appearance of the solution becomes more transparent visibly. Complete visible transparency occurs at pH 2.5 (point F) and reveals the highly defined hypersensitive characteristic absorbance bands of Nd(III). We can assume that at this point, NP aggregation has been significantly enough reduced since scattering losses are



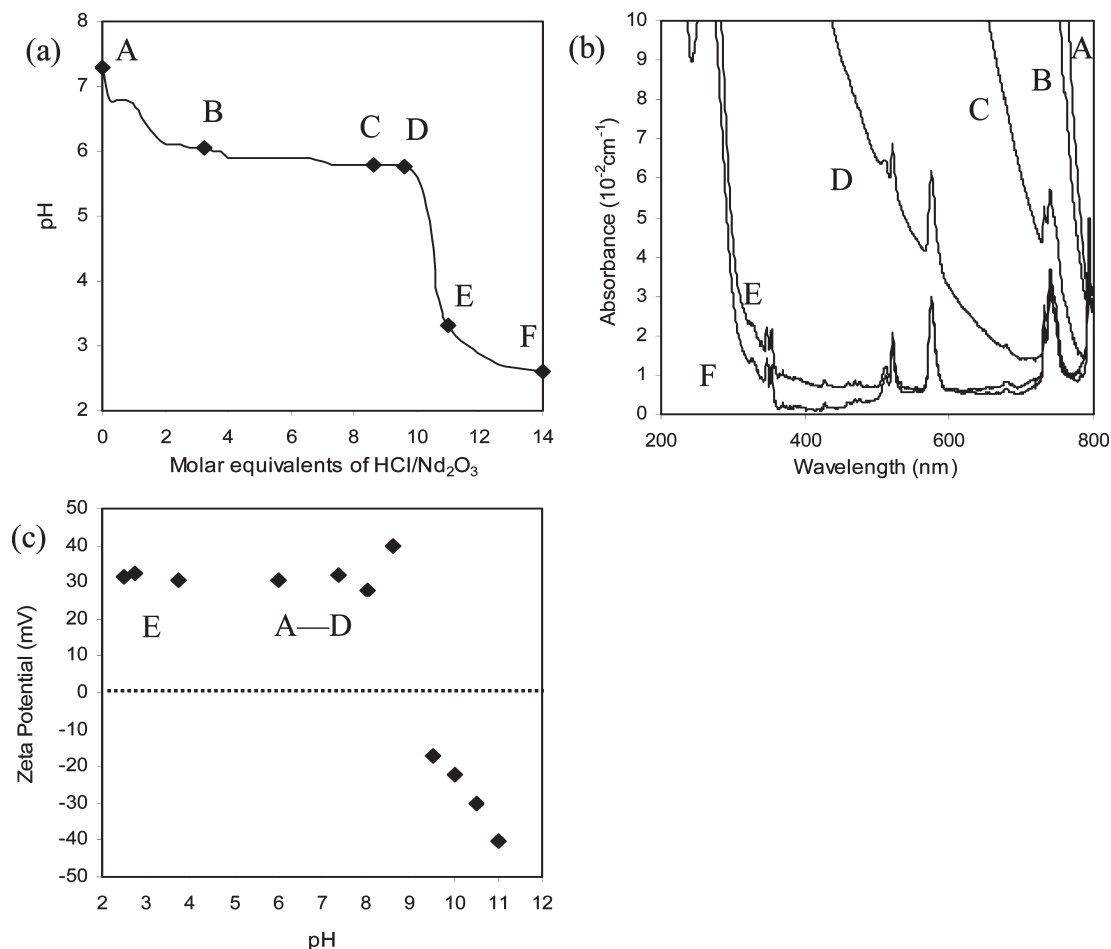


**Figure 2.** (a) pH titration curve of Nd<sub>2</sub>O<sub>3</sub> NPs; (b) UV-vis spectra of the corresponding A–F aliquots withdrawn at different times of the titration; (c) surface charge measurements of Nd<sub>2</sub>O<sub>3</sub> NPs under different pH conditions.

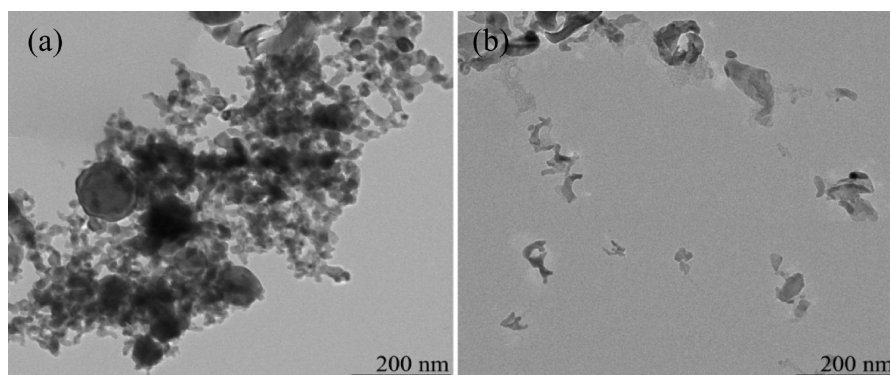
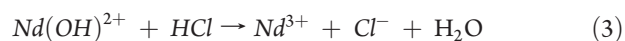
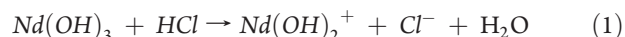


**Figure 3.** TEM images of (a) Nd<sub>2</sub>O<sub>3</sub> NPs aggregated (A, pH 7.5), and (b) dispersed (F, pH 2.5).

absent in the spectrum. Figure 3b further supports this observation, as aggregates of smaller dimensions (30 and 100 nm) appear under lower pH conditions.

Nanoparticle dispersion can be rationalized by examining the chemical reactions that occur at the particle surface when HCl is added to the solution. The hydroxyl groups at the Nd<sub>2</sub>O<sub>3</sub> NP surfaces which were formed upon hydration gradually react with the acid to release water molecules, while the carbonate surface groups quickly respond to the acid by liberating CO<sub>2</sub> molecules,

exposing fresh hydroxyl groups at the surface. The acid reaction is very slow and reaches three equilibrium states:



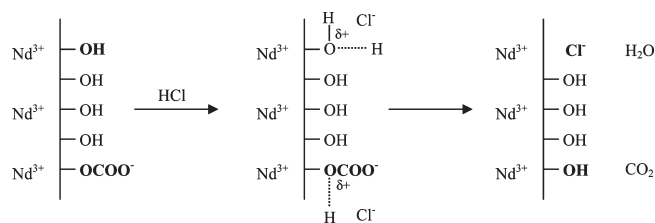


**Figure 4.** Proposed mechanism for the surface reactivity of neodymium oxide NPs with HCl.

The two hydroxylated ionic species from eqs 1 and 2 are present in solution above pH 5 (region between A and D), whereas the trivalent neodymium ionic form, eq 3, is dominant below pH 2.5 (region below F). In the presence of a slight excess of HCl, neodymium forms only weak complexes with chloride at room temperature<sup>31,32</sup> and has a high tendency to hydrolysis. Indeed,  $\text{Nd}^{3+}$  is known to coordinate to nine water molecules in solution in a tricapped-trigonal prism arrangement.<sup>33</sup> eqs 1–3 suggest that a positive charge forms at the crystal surface upon acidification. These assumptions are confirmed by the surface charge measurements provided in Figure 2c, which display positive zeta potential values when the pH is below 8. Above that pH a charge reversal is observed and attributed to the deprotonation of the surface hydroxyl groups. From theoretical calculations, a total of 6 mols of HCl is required to complete the reaction. However the titration results indicate that almost 10 mols of acid were added at the neutralization point. It is worth noting that the rate of dissolution of neodymium oxide is very slow and depends largely on the surface of contact between the NPs, the water and the acid. Because of the initial aggregation state of the NPs, surface reactions may therefore be highly restricted and less frequent. For that reason, rare earth oxides are usually heated upon dissolution to promote the reaction.

A proposed mechanism of nanoparticle dispersion based both on these theoretical considerations and on the acquired experimental information, is described as follows: Protons, as they are added to the NP suspension first adsorb onto the NPs surface active sites, which include oxygen bridges, carbonate groups and hydroxyl groups, via H-bonding and electrostatic interactions. They progressively react with these groups to form  $\text{CO}_2$  and water molecules. The proposed mechanism is illustrated in Figure 4. The initially high aggregation state of NPs slows down the reaction, which consequently requires excess acid to be driven more efficiently. In the process, the aggregate sizes are reduced as confirmed by Figure 3b, which in turn reduces visible scattering (Figure 2b). The reduction in dimension is significant enough so that complete visible transparency is reached at pH 2.5. At this point, there is a large excess of acid in solution that suggests complete ionizations of neodymium NPs. However, the fact that a positive surface potential is still detectable at pH 2.5 and that small neodymium clusters are still visible by TEM, clearly indicates that NPs are still present in solution to a certain extent. Due to the impractically low pH required, and the tendency of neodymium to complex with chlorine atoms or to form hydrolyzed compounds under strongly acidic conditions, it is difficult to determine what fraction of ionized species are present in solution or their nature. Because of these limitations, the use of acidification to very low pH to disperse NPs is therefore not recommended.

Because of the possibility of soluble Nd compounds existing in the solution at low pH, it is not possible to draw conclusions

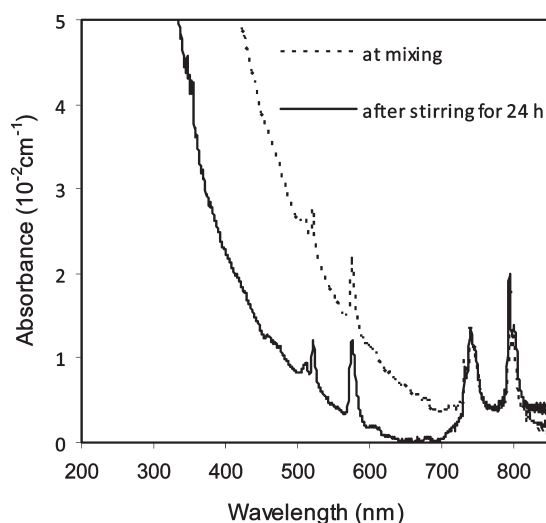


**Figure 5.** UV-visible absorbance spectra of a mixture of PAH and  $\text{Nd}_2\text{O}_3$ .

from Figure 2b concerning the effective absorption of the nanoparticles as opposed to dissolved compounds. Therefore it is not possible to determine whether the use of nanoparticles would improve the absorption in the region of interest between 350 and 450 nm for the SNO+ experiment.

**Interactions of  $\text{Nd}_2\text{O}_3$  NPs with Polyelectrolytes.** Next, we investigate the colloidal behavior of the  $\text{Nd}_2\text{O}_3$  as a function of pH and in the presence of two structurally different polyelectrolytes; a weak polycation, PAH and a strong polyanion, PSS. The objective is to determine if such polyelectrolytes can efficiently disperse and stabilize the neodymium oxide NPs through repulsive or attractive interactions, without favoring ionization but respecting transparency criteria.

**Interactions with Poly(allylamine hydrochloride).** Poly(allylamine hydrochloride) (PAH), a weak polycation inexpensive and readily available, is employed extensively in the fabrication of polyelectrolyte multilayer films (PEMs) and in the electrostatic stabilization of colloidal systems. PAH is generally used to stabilize oppositely charged substrates via electrostatic attraction and overcharging effect, but in the current work the polymer is expected instead to act as a repulsive dispersant as it carries the same charge as the neodymium oxide NPs. The addition of PAH to the neodymium oxide aggregated mixture however led to an unexpected phenomenon as the polymer appeared to have chemical affinity to the surface of neodymium oxide NPs. This unusual response was reflected by the high transparency of the solution, which occurred after a large amount of PAH was mixed with the colloidal suspension. Hence, the acidic protons of the amino groups of PAH, may be able to react with the neodymium suspension in a similar manner to that of HCl. From calculated estimates, a number approximated to 45 equivalents of PAH monomer per  $\text{Nd}_2\text{O}_3$  particle was required to achieve the highest degree of visible transparency for that particular mixture.

The UV-visible absorbance spectrum of the mixture is presented in Figure 5 and was recorded for two different mixing times. These results clearly suggest that the reaction might be slow as a longer mixing time yields a higher transparency, although not useable in the critical region of application between 350 and 450 nm. Contrary to the acidification process which

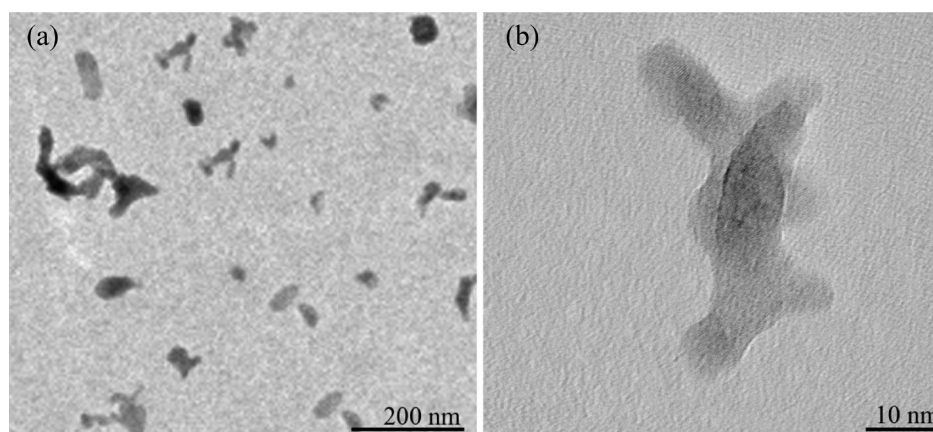


**Figure 6.** TEM images of the PAH and  $\text{Nd}_2\text{O}_3$  mixture, showing (a) a majority of dispersed NPs and only few aggregates, and (b) an example of complex particle morphology.

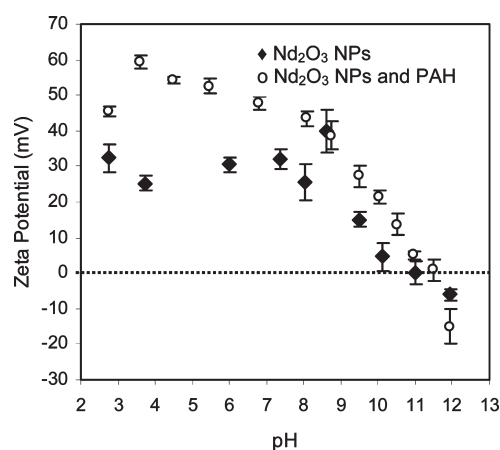


**Figure 7.** Zeta potential of a mixture of PAH and  $\text{Nd}_2\text{O}_3$  recorded at different pH.

provides fairly high transparency at pH 2.5, a certain degree of scattering below 600 nm is still observable however even after a high excess of polymer was added. It is worth mentioning that the presence of excess polyelectrolytes did not alter the pH of the solution which was kept to a constant pH of 6.8 at any time during the polymer addition. This lack of pH fluctuation results from the high buffer capacity of PAH whose  $\text{pK}_a$  is about 8.6. Therefore, the solution acidity may play an important role in the reaction process between the neodymium oxide and protons that is closely related to the solution transparency. On the other hand, by maintaining the solution at a higher pH value it becomes easier to avoid the undesirable neodymium ionization that occurs under acidic conditions. TEM images presented in Figure 6 clearly demonstrate that the presence of PAH contributes to the NP dispersion, as the micrometer size  $\text{Nd}_2\text{O}_3$  aggregates are no longer visible and are replaced by particles of smaller dimensions whose sizes range between 10 and 50 nm, with the 2 size extremes being visible by electron microscopy. The particle polydispersity is still appreciable however, considered qualitatively as a size range observed to be 5-fold, and the particle morphologies can be complex. Few polymer/particle aggregates were also found on the surface of the TEM grid which may contribute to the residual scattering in the absorbance spectrum.

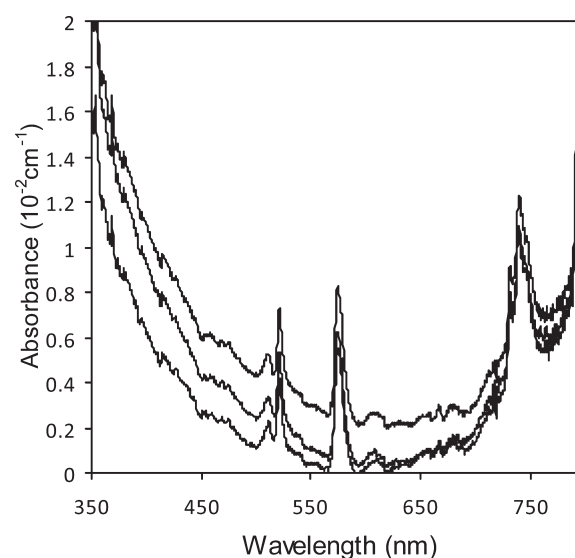


**Figure 8.** UV-visible absorbance spectra of a neodymium and PAH mixture further acidified with 0.1 M HCl. The absorbance curves, from bottom to top, correspond to pH 2.7, 4.5, and 6.3, respectively.

Figure 7 suggests that the presence of PAH also significantly alters the surface potential of the bare  $\text{Nd}_2\text{O}_3$  NPs, as the polycation induces an increase in magnitude of the surface charge of about 25 mV at the pH of mixing. This effect is amplified as the pH of the solution is lowered. Since the pH reduction is achieved by HCl addition, an improvement in transparency is also observed under lower pH conditions (Figure 8). It is worth noting that magnitude of absorbance values are particularly low compared to previous neodymium results; however, this reduction might be attributed to dilution rather than transparency improvement. The correlation between the solution acidity and transparency is therefore confirmed. On the other hand, increasing the pH of the solution induces a gradual decrease of the magnitude of the surface charge potential toward zero. Total charge neutralization is reached at around pH 11, and colloidal precipitation occurs in the vicinity of the point of zero charge (ZPC) of the polymer, which is at pH 10. We speculate that insufficient repulsive interaction between colloid and polymer may be the primary reason for precipitation. For comparison

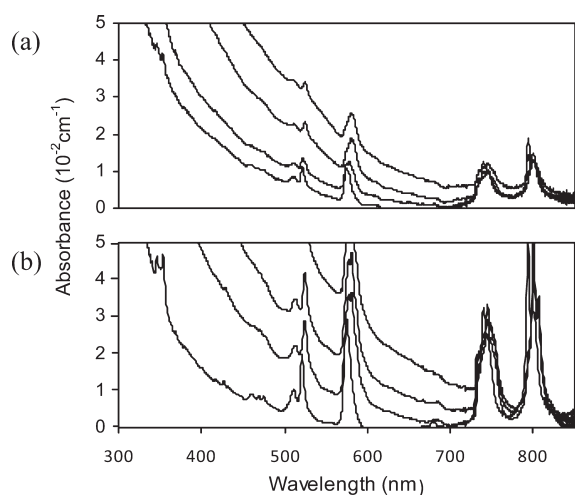


**Figure 9.** Absorbance spectra of the  $\text{Nd}_2\text{O}_3$  NPs made basic with NaOH in the (a) presence and (b) absence of PAH. The absorbance curves, from bottom to top, correspond to pH 6.5, 8, 9, and 10.5, respectively.

purposes, the pure  $\text{Nd}_2\text{O}_3$  NPs were also acidified until transparent and then neutralized with NaOH. In the case of the pure material, precipitation was also observed at a similar pH. Therefore, the precipitation source may not only be related to the polymer charge neutralization, as bare NPs experience the same charge neutralization under basic conditions.

Alkanization has also been monitored by absorbance spectroscopy for the two colloidal systems (Figure 9). The absorption band of Nd(III) at 575 nm, which has been widely used in the study of metal–ligand complexation due to its high sensitivity to variations in strength of complexation<sup>21</sup> was carefully examined. In both cases, a shift of this band toward longer wavelengths is observed and is also accompanied by an increase in peak intensity. The red shift indicates that a stronger complexation takes place between the neodymium atom and any incoming ligand, while an increase in intensity is attributed to aggregation. In the case where bare  $\text{Nd}_2\text{O}_3$  NPs were made basic, hydroxide ions were the only possible source of precipitation. Previous literature reports have for that matter confirmed that the blue gelatinous precipitate that forms upon NaOH addition is due to the complexation between the trivalent neodymium atoms and the hydroxyl groups.<sup>34</sup> The precipitation only takes place at a pH that is sufficiently far from the  $\text{p}K_a$  (8.6) of this water-insoluble hydrous oxide. Due to the limited availability of information on the nature and distribution of neodymium species that were formed at low pH, it is not clear exactly how the complexation with the NaOH takes place. In the case where we consider that the neodymium oxide NPs are still present, then the complexation can only occur at the nanoparticle surface. On the other hand, we speculate that if the possibility that some neodymium ions are present in their ionic form is taken into account, then the complexation may take place at the atomic level at all sites. In the case where PAH was present in the colloidal mixture, possible coprecipitation may have occurred because the PAH  $\text{p}K_a$  coincides with that of the hydrous neodymium oxide. FTIR and TGA analysis of the blue precipitate have confirmed that some polymers remained in association with the neodymium particles. Because the polycation gradually becomes uncharged above pH 8.6, it is also possible that the unprotonated amino groups are

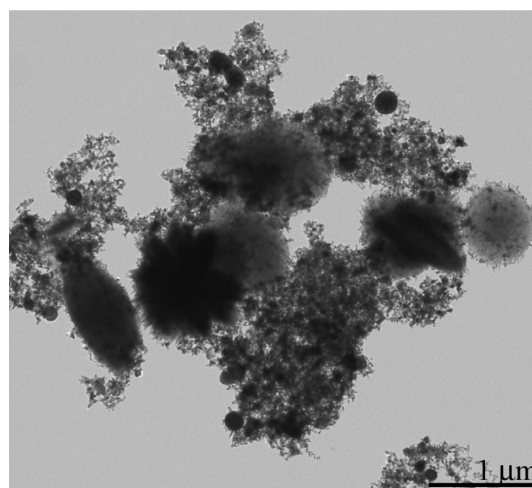


**Figure 10.** TEM image of a mixture of PSS and  $\text{Nd}_2\text{O}_3$  (pH 9).

being involved in some kind of H-bonding with the neodymium compound.

A proposed mechanism for the dispersion of the neodymium NPs by PAH is very similar to that of the acidification with HCl except that the reaction with the polymer is less vigorous, and some residual scattering is always present even after excess polymer is added. Solution transparency is therefore limited to the region of the visible spectrum that is above 600 nm. The less acidic character of protonated PAH may contribute to this discrepancy. On the other hand, the buffer capacity of the polymer is very advantageous as neodymium ionization is more easily reduced or eliminated. The use of this polymer to disperse neodymium oxide NPs is therefore a good alternative to HCl, which become problematic in the region of pH of transparency. The range of stability of the NPs is however limited as NPs precipitate when exposed to higher pH conditions (pH above 10). This is also true for the neodymium NPs acidified with HCl. It is also important to mention other possible contributing roles that lead to the complexation of the PAH to the NPs, such as hydrophobic interactions, or shifts in the effective  $\text{p}K_a$  values of PAH when adsorbed to a surface, altering the surface interactions.<sup>16</sup>

**Interactions with Poly(4-styrene sulfonate).** Previous work on poly(styrene sulfonate) films doped with Nd(III) at neutral pH have demonstrated that an effective interaction of coordination takes place between a trivalent neodymium ion and three sulfonate groups belonging to three different monomers of PSS.<sup>24</sup> These observations were reported for low pH conditions where the polymer is uncharged and the neodymium atom is fully ionized. In this work, the potential of interaction between PSS and the neodymium is also studied but under conditions where both the polymer and the neodymium NPs surfaces are charged. Thus, in this different context where the polymer carries a charge opposite to the neodymium NP surface charge, it becomes possible to exploit electrostatic attractive interactions to disperse and stabilize the aggregated suspensions.

In contrast to the addition of PAH, which drastically reduces the size of aggregates, the presence of PSS in the mixture does not seem to affect the stability of the colloidal solution as its high aggregation state is preserved. However, TEM images such as that in Figure 10 reveal that some parts of the colloidal network



seem to interact with the polymer as amorphous spheres are formed around some aggregated sites. The existence of electrostatic interactions between the polymer and the NP surfaces appear more obvious when examining the zeta potential measurements, presented in Figure 11. Results reveal that in the presence of PSS, the net charge at the neodymium NPs surface is reversed, confirming significant electrostatic interactions between the two coexisting species.

To reduce the aggregate size and induce particle dispersion, the mixture was further acidified with HCl until transparency. Figure 11 clearly shows that the charge reversal is preserved under acidic pH conditions and Figure 12 shows that NP sizes are reduced. Under these acidic pH conditions however, an unknown percentage of ionized neodymium might also be present. The range of pH stability of these acidified NPs was also investigated by gradually increasing the pH of the solution with NaOH. Absorbance spectra were recorded at different stages of the reaction (figure 13) and reveal that in contrast to the acidified  $\text{Nd}_2\text{O}_3$  NPs and the  $\text{Nd}_2\text{O}_3$ /PAH mixture, the alkanisation of the  $\text{Nd}_2\text{O}_3$ /PSS mixture (preliminary acidified), did not cause any nanoparticle precipitation. This is also reflected by the preserved transparency and the absence of increase in absorbance peak intensity. TEM images also reveal that the NP small sizes are preserved upon alkanization and that isolated particles as small as 5 nm in diameter were found on the surface of the TEM grid. Therefore, it appears that the presence of PSS in solution

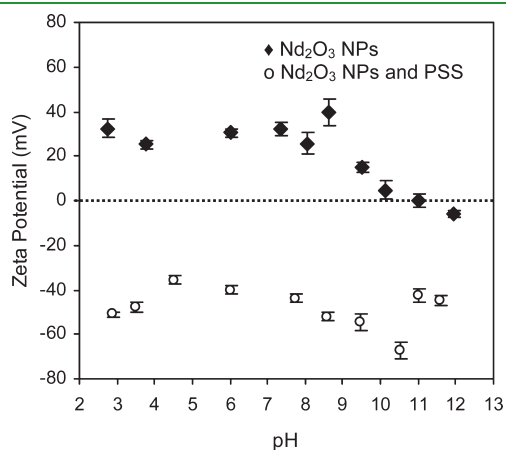


**Figure 11.** Zeta potential of a mixture of PSS and  $\text{Nd}_2\text{O}_3$  recorded at different pH values.

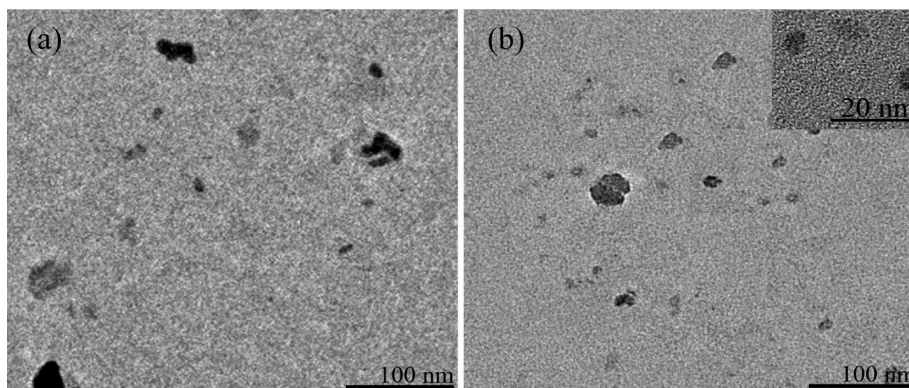


**Figure 12.** TEM image of PSS and  $\text{Nd}_2\text{O}_3$  mixture at (a) pH 2.8 and (b) pH 10.

hinders the complexation between the hydroxyl ions and the particle surface. Electrostatic interactions between the polyanion and the positively charged particles may be responsible for this interesting phenomenon. A red shift of all absorbance peaks is, however, observed as the solution becomes more basic, indicating an increase in the complexation strength between the neodymium and its ligand. One hypothesis for this is that under basic conditions, chlorine ions which remained associated to the neodymium NPs surfaces from the previous acidification, associate with sodium ions. Thus, interactions between the neodymium and PSS sulfonate groups are becoming stronger as fewer chlorine atoms are available for competing for neodymium adsorption sites. Therefore, PSS becomes a very efficient stabilizing agent for neodymium nanoparticles when such NPs are acidified in the presence of the polymers, reducing absorbance for many wavelengths. Inherent Nd absorbance drawbacks specific to the SNO+ application wavelength criteria will be outlined in the conclusions. Under these conditions, however, PSS can associate with the NP surfaces to provide them good protection against hydroxyl complexation at higher pH. High solution transparency and small nanoparticle dimensions are also preserved under a large range of pH values, over a wide range of wavelengths.

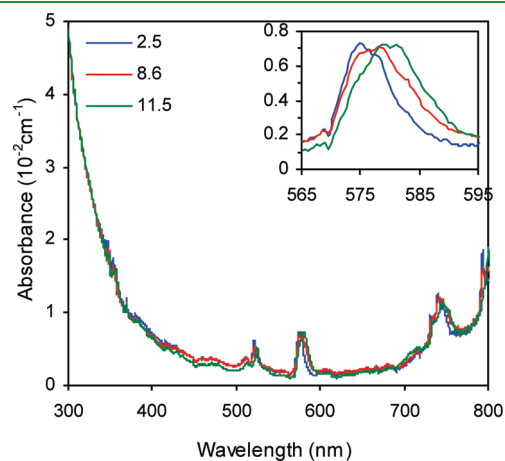


**Figure 13.** Absorbance spectrum of the  $\text{Nd}_2\text{O}_3$  suspension in the presence of PSS. The mixture was first acidified with HCl to pH 2.5 and then made basic with NaOH until 11.5. Red shift in absorbance upon alkanization is illustrated in the enlarged section between 565 and 595 nm.



## CONCLUSION

In summary, conditions were found whereby the colloidal behavior of Nd<sub>2</sub>O<sub>3</sub> NPs can be significantly controlled by the solution pH, and to promote good particle dispersion and increase visible transparency. Acidic conditions were found best to induce the fragmentation of large aggregates into smaller size particles and favor their dispersion, whereas the highest pH values generated particle precipitation. High solution transparency is only achieved under strongly acidic conditions however where the neodymium oxide particle integrity may begin to be compromised. Indeed, high acid concentration can favor the dissolution of neodymium NPs into its ionized and soluble form, which exhibit typical absorbance lines in the spectral region of interest. The fraction of ionized species and their chemical identities are still unknown, but the addition of PAH can solve this problem because the polymer has the faculty to disperse the particles at a pH closer to neutrality. The transparency region above 600 nm is still good. The NP dispersion stability is also restricted to neutral pH ranges as precipitation occurs at pH 10. The use of PSS alone does not induce dispersion at neutral pH conditions, as subsequent acidification is required to reduce the size of aggregation and to obtain solution transparency. In contrast to PAH, the polymer associates more strongly to the neodymium surface which makes the suspension stable over a larger pH range. Therefore, the use of polyelectrolytes to disperse neodymium oxide NPs can be advantageous in the case where the formation of ionized species is to be avoided and for situations where suspensions need to be prepared under non-acidic conditions. This work to determine the surface chemistry, and initial conditions for optimization of transparency was performed in aqueous media. Eventual applications will require the dispersed Nd NPs to be transferred to LAB or similar scintillation solvents, but work is ongoing to pursue various transfer techniques with some encouraging preliminary success, and will be the subject of future manuscripts. Also, although transparency has been shown to be improved substantially in these aqueous studies over wide wavelength regions; however, optical visibility has not been improved in the region of highest interest since the undesirable absorbance lines exhibited by neodymium itself were still present and comparable in intensity to dissolved neodymium. Consequently, this stabilization strategy is not yet directly suitable for the proposed particle physics application, but again further investigations are being undertaken currently to solve this issue, and we regard the results described here as an encouraging first step in this large project.

## AUTHOR INFORMATION

### Corresponding Author

\*E-mail: christopher.barrett@mcgill.ca.

## ACKNOWLEDGMENT

The authors acknowledge McGill Undergraduate Chemistry students Sophie Ault and Valentina Licursi for helpful experimental assistance to this work, as well as Dr. David Liu, McGill Physics for TEM image assistance. We are grateful for project funding from NSERC Canada, CSACS the Centre for Self-Assembled Chemical Structures McGill, and to SNO+ Canada. Prof. A.M. Herzberg is thanked for facilitating initial project discussions with a travel grant to the 9th SSPP conference, Herstmonceux, U.K.

## REFERENCES

- (1) Que, W.; Kam, C. H.; Zhou, Y.; Lam, Y. L.; Chan, Y. C. *J. Appl. Phys.* **2001**, *90*, 4865–4867.
- (2) Singh, J.; Soni, N. C.; Srivastava, S. L. *Bull. Mater. Sci.* **2003**, *26*, 397–399.
- (3) Delmore, F.; Harnois, C.; Monot-Laffez, I.; Desgardin, G. *Physica C* **2002**, *372*, 1127–1130.
- (4) Tosun, G.; Rase, H. F. *Ind. Eng. Chem. Prod. Res. Dev.* **1972**, *11*, 249–260.
- (5) Chevalier, S.; Bonnet, G.; Larpin, J. P. *Appl. Surf. Sci.* **2000**, *167*, 125–133.
- (6) Sayle, T. X. T.; Parker, S. C.; Sayle, D. C. *Phys. Chem. Chem. Phys.* **2005**, *7*, 2936–2941.
- (7) Zawadzki, M.; Kepinski, L. *J. Alloys Compd.* **2004**, *380*, 255–259.
- (8) Kepinski, L.; Zawadzki, M.; Mistra, W. *Solid State Sci.* **2004**, *6*, 1327–1336.
- (9) Boger, J.; Hahn, R. L.; Rowley, J. K.; Carter, A. L.; Hollebone, B.; Kessler, D.; Blevis, I.; Dalnoki-Veress, F.; DeKok, A.; Farine, J. *Nucl. Instrum. Methods Phys. Res., Sect. A* **2000**, *449* (1–2), 172–207.
- (10) Ahmad, Q. R.; Allen, R. C.; Anderson, T. C.; Anglin, J. D.; Barton, J. C.; Beier, E. W.; Bercovicth, M.; Bigu, J.; Biller, S. D.; Black, R. A. *Phys. Rev. Lett.* **2002**, *89* (1–6), 011301.
- (11) Yu, R. B.; Yu, K. H.; Wei, W.; Xu, X. X.; Qiu, X. M.; Liu, S.; Huang, W.; Tang, G.; Ford, H.; Peng, B. *Adv. Mater.* **2007**, *19*, 838–842.
- (12) Rill, C.; Bauer, M.; Bertagnolli, H.; Keickelbick, G. *J. Colloid Interface Sci.* **2008**, *325*, 179–186.
- (13) Decher, G.; Hong, J. D.; Schmitt, J. *Thin Solid Films* **1992**, *210/211*, 831–835.
- (14) Rodriguez, L. N. J.; De Paul, S. M.; Barrett, C. J.; Reven, L.; Spiess, H. W. *Adv. Mater.* **2000**, *12* (24), 1934–1938.
- (15) Dorris, A.; Rucareanu, S.; Reven, L.; Barrett, C. J.; Lennox, R. B. *Langmuir* **2008**, *24*, 2532–2538.
- (16) Burke, S. E.; Barrett, C. J. *Biomacromolecules* **2005**, *6*, 1419–1428.
- (17) Tanchak, O. M.; Barrett, C. J. *Chem. Mater.* **2004**, *16*, 2734–2739.
- (18) Ohno, H.; Peng lau, S. *Polym. Adv. Technol.* **1991**, *2*, 103–107.
- (19) Okamoto, Y.; Ueba, Y.; Dzhanibekov, N. F.; Banks, E. *Macromolecules* **1981**, *14*, 17–22.
- (20) Banks, E.; Okamoto, Y.; Ueba, Y. *J. Appl. Polym. Sci.* **1980**, *25*, 359–368.
- (21) Lis, S.; Wang, Z.; Choppin, G. R. *Inorg. Chim. Acta* **1995**, *239*, 139–143.
- (22) Montavon, G.; Grambow, B. *New J. Chem.* **2003**, *27*, 1344–1352.
- (23) Silva, M. C.; Cristovan, F. H.; Nascimento, C. M.; Bell, M. J. V.; Cruz, W. O.; Marletta, A. *J. Non-Cryst. Solids* **2006**, *352*, 5296–5300.
- (24) Cristovan, F. H.; Nascimento, C. M.; Bell, M. J. V.; Laureto, E.; Duarte, J. L.; Dias, I. F. L.; Cruz, W. O.; Marletta, A. *Chem. Phys.* **2006**, *326*, 514–520.
- (25) Schneider, G.; Decher, G. *Nano Lett.* **2004**, *4*, 1833–1839.
- (26) Caro, P.; Derouet, J.; Beaury, L. *J. Chem. Phys.* **1979**, *70*, 2542–2549.
- (27) Kang, Z. C.; Eyring, L. *Aust. J. Chem.* **1996**, *49*, 981–996.
- (28) Antic-Fidancev, E.; Holsa, J.; Lastusaari, M. *J. Alloys Compd.* **2002**, *341*, 82–86.
- (29) Nagao, M.; Hamano, H.; Hirata, K.; Kumashiro, R.; Kuroda, Y. *Langmuir* **2003**, *19*, 9201–9209.
- (30) Bernal, S.; Blanco, G.; Calvino, J. J.; Perez Omil, J. A.; Pintado, J. M. *J. Alloys Compd.* **2006**, *408–412*, 496–502.
- (31) Moeller, T.; Brantley, J. C. *Anal. Chem.* **1950**, *22*, 433–441.
- (32) Migdisov, A. A.; Williams-Jones, A. E. *Geochim. Cosmochim. Acta* **2002**, *66*, 4311–4323.
- (33) D'angelo, P.; Pavel, N. V.; Borowski, M. *J. Synchrotron Rad.* **2001**, *8*, 666–668.
- (34) Moeller, T.; Kremers, H. E. *Chem. Rev.* **1945**, *37*, 97–159.